Available online at www.sciencedirect.com
ScienceDirect
Geochimica et Cosmochimica Acta 73 (2009) 6084–6097
Geochimica et Cosmochimica Acta
www.elsevier.com/locate/gca

Boron isotopes geochemistry of the Changjiang basin rivers

B. Chetelat [a,*], C.-Q. Liu [a,*], J. Gaillardet [b], Q.L. Wang [a], Z.Q. Zhao [a], C.S. Liang [a], Y.K. Xiao [c]

[a] State Key Laboratory of Environmental Geochemistry, Institute of Geochemistry, CAS, 46 Guanshui Road, 550002 Guiyang, PR China
[b] Equipe de Géochimie et Cosmochimie, Institut de Physique du Globe de Paris, Université Paris 7, UMR 7579, 4 place Jussieu, 75252 cedex 05, France
[c] Qinghai Institute of Salk Lakes, Chinese Academy of Sciences, Xining, Qinghai 810008, PR China

Received 20 January 2009; accepted in revised form 20 July 2009; available online 28 July 2009

Abstract

We report analyses of B isotopic compositions in water and suspended particulate matter collected in the Changjiang and its main tributaries. We showed that four sources control the dissolved boron budget; namely atmospheric deposition, evaporite dissolution, anthropogenic inputs and silicate weathering. The contribution of silicate weathering to the dissolved B load ranges from 40% to 50% for the Changjiang main channel and from 45% to 88% for the main tributaries. The isotopic composition of dissolved boron derived from silicate weathering range from −3‰ up to +9‰ suggesting that isotopic fractionation occurs during silicate weathering. The boron isotopic composition of suspended particulate matter range from −11.4‰ to −6‰. Boron derived from silicate weathering is preferentially carried out by the dissolved load which accounts for 30–96% of the total boron. We show that the isotopic compositions of both the dissolved load and suspended particulate matter are controlled by the competition between boron leaching and boron uptake into secondary phases. The first process is characterized by a loss of boron relative to the bedrock without apparent isotopic fractionation whereas the last one is associated to a large isotopic fractionation which enriches the dissolved boron in heavy isotope.

1. INTRODUCTION

Changes in silicate weathering rate have the potential to regulate atmospheric CO_2 level and thus climate at geological timescales (Berner et al., 1983; Raymo et al., 1988; Godderis and Francois, 1995; Godderis et al., 2003). Hence, quantification of silicate weathering rates deduced from the study of large rivers and identification of their controls such as climatic, tectonic factors at the present day are essential to interpret paleo-records and reconstruct past climatic changes.

In this aim, during the last years, efforts have been made to develop new isotopic tracers such as Li, Si, Ca, and Mg (Huh et al., 2001; Kisakurek et al., 2005; Georg et al., 2006; Tipper et al., 2006) for the study of chemical weathering. Boron isotopes may also be of interest, but further studies are required to understand the B isotopes behaviour during continental weathering.

As boron exhibitits a single oxidation state in nature, isotopic fractionation between its two stable isotopes ^{10}B (20%) and ^{11}B (80%) is caused by changes in its coordination number or the ligands present in its coordination sphere (Lemarchand et al., 2007). Such changes may occur when aqueous boron present in dilute solution as trigonal boric acid (pKa = 9.23 at 25 °C, Baes and Mesmer, 1976) and tetrahedral borate ion which is enriched in light isotope by around 30‰ (Byrne et al., 2006) compared to the trigonal species, adsorbs at solid surfaces or coprecipitates in solids.

It has been demonstrated that boron isotopes are fractionated during adsorption onto clays (Palmer et al., 1987; Spivack et al., 1987), humic acids (Lemarchand et al., 2005; Tossell, 2006) and Fe/Mn oxides (Lemarchand et al., 2007)

* Corresponding authors.
E-mail addresses: benjamin@vip.gyig.ac.cn, b.chetelat@yahoo.com (B. Chetelat), liucongqiang@vip.skleg.ac.cn (C.-Q. Liu).

0016-7037/$ - see front matter © 2009 Elsevier Ltd. All rights reserved.
doi:10.1016/j.gca.2009.07.026

and that the isotopic fractionation factor was pH dependant. These experimental results highlight the potential use of boron isotopes in studies related to chemical weathering but up to now, field studies are scarce and mainly focused on the dissolved load of rivers (Spivack et al., 1987; Rose et al., 2000; Lemarchand et al., 2000, 2000a,b; Lemarchand and Gaillardet, 2006). Based on the analysis of the dissolved load of some Himalayan rivers, Rose et al. (2000) proposed that the huge range of $\delta^{11}B$ (from −7‰ to +37‰) reflected the isotopic composition of soil solutions and that the river water would preserves a record of the pH conditions during B coprecipitation/adsorption in/onto secondary clays. Spivack et al. (1987) reported the B isotopic compositions measured along a soil profile in the Orinoco Basin and showed that the mobilization of boron during silicate weathering was accompanied by a slight isotopic fractionation (less than 3‰) that the authors explained by the selective dissolution of primary minerals.

Recently, Lemarchand and Gaillardet (2006) studied the B isotopic of the dissolved load from rivers of the Mackenzie basin. As for Himalayan rivers (Rose et al., 2000), the range of isotopic composition covers a large range of variation from −2‰ to +30‰. The authors showed that dissolved B in rivers was regulated by input of groundwaters and that its isotopic composition is controlled by hydrological conditions, shales weathering rates and by interactions between aqueous boron and solid surfaces. They concluded that the B geochemical cycle for the Mackenzie basin was not at a steady state and that the present B fluxes responded to past changes of the water/rock interactions.

Because boron is soluble and partitioned between dissolved and solid loads, study of solid material carried by rivers should provide some information on boron isotope behaviour during chemical weathering. Until now, no systematic study has been carried out on the boron isotopic composition of riverine sediments and we report here the first study on B isotopic geochemistry for both dissolved and solid loads of a large riverine system, the Changjiang basin. Major elemental and strontium isotopic compositions of the water river analyzed in this paper were previously reported by Chetelat et al. (2008). In this article, we used a series of elemental chemical ratios coupled with the Sr isotopic compositions of the dissolved load to distinguish between inputs from weathering, pollution and rainwater. Results showed that the rivers chemistry was dominated by carbonate weathering with the exception of the Changjiang Upper Reach displaying a high contribution of evaporite weathering and a couple of singular rivers like the Ganjiang dominated by silicate weathering and anthropogenic inputs. We showed that the cation-silicate weathering rate was highly variable from one sub-basin to another and varies by more than one order of magnitude, ranging from 0.7 to 7.1 t/km^2/yr. For the Changjiang main channel, the rate calculated at different sampling sites slightly increases from upstream to downstream. This article also highlighted the relative important contribution of anthropogenic inputs to the water chemistry and we estimated that they contributed between 15% and 20% to the cationic TDS (Total Dissolved Solids) for the Changjiang main channel.

The aims of this paper are to decipher the sources of boron in the river water, especially to evaluate the role of silicate weathering on the boron budget and investigate the behavior of its isotopes during chemical weathering by analyzing the isotopic composition of both dissolved and suspended solid loads.

2. NATURAL SETTINGS OF THE CHANGJIANG DRAINAGE BASSIN

The Changjiang drainage basin covers a total area of 181×10^4 km^2, about 1/5 of China (Fig. 1) and with a length of 6300 km, the Changjiang is the 3rd longest river in the world. From its source in the Qinghai–Tibet Plateau to the East China Sea, the Changjiang has a fall of over 5400 m. The Changjiang watershed is mainly overlain by sedimentary rocks (Fig. 2) composed of marine carbonates, evaporite and alluvium from Precambrian to Quaternary in age. Carbonate rocks are widely spread over the basin and are particularly abundant in the southern part (Yunnan, Guizhou and western Hunan Provinces) and the sub-basin of the Hanjiang (Chen et al., 2002) (Fig. 2). Evaporitic deposits are mainly present in the Upper Reach of the Changjiang whereas rivers of the Poyang Lake sub-basin drain mainly metamorphic and igneous rocks (Fig. 2).

With the exception of the source area characterized by high elevation and cold climate, the Changjiang basin has a subtropical monsoon climate, temperate and humid (mean temperature 16–18 °C for the Middle and Lower Reaches). The yearly rainfall amount averages 1100 mm and is unevenly distributed, decreasing gradually from southeast to northwest, from 1644 mm/yr for the Lower Reach and 1396 mm/yr for the Middle Reach to 435 mm/yr for the Upper Reach (Chen et al., 2001). Surface runoff is the major water supply or the Changjiang watershed, accounting for 70–80% of the total water discharge (Chen et al., 2002).

Floods in the Changjiang basin are formed by storms concentrated during the period from May to October. The rainy season occurs earlier in the Middle and Lower Reaches than in the Upper Reach, the earliest affecting the Dongting Lake and Poyang Lake systems between April and July. The amount and distribution in both time and space of rainfall in the wet season directly impacts the sediment amounts, the sediments discharge being concentrated during the rainy season. Before the completion of the Three Gorges Dam project, the suspended load averaged 434×10^6 t/yr at Yichang and 352×10^6 t/yr at Datong, the most downstream control station not marked by tidal influence, during the period 1986–1998 (Yang et al., 2002a).

The Changjiang basin is highly populated, about 35% of the national population lives there and the mean population density is around 226 h/km^2 (Liu et al., 2003). Population is unevenly distributed and mainly concentrated in the Sichuan basin, the Middle and Lower Reaches. The natural vegetation is mainly distributed in the mountainous and hilly areas whereas cultivated landscapes prevail in the plain. The cultivated land represents about 13% of the watershed mainly located in the Sichuan basin, the Middle and

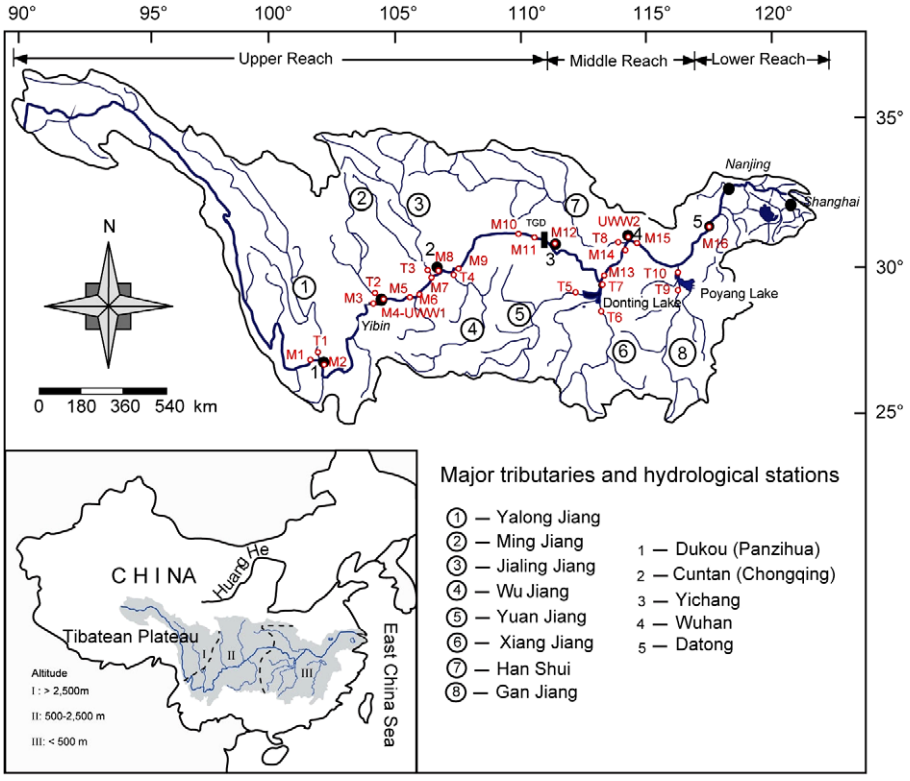

Fig. 1. Changjiang watershed and samples location.

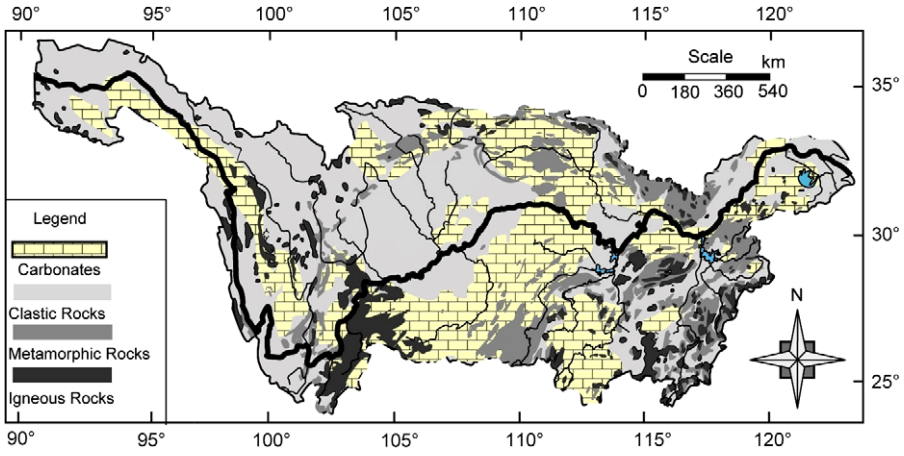

Fig. 2. Geological map of the Changjiang watershed.

Lower Reaches (Xing and Zhu, 2002). Due to the high level of development of the valley, pollution is a crucial issue for the Changjiang watershed (Fu et al., 2007) which collects the domestic/industrial wastewater and field waters.

3. SAMPLING AND ANALYTICAL METHODS

3.1. Samples collection and preparation

Samples were collected in August 2006 along the Changjiang main channel and its main tributaries (Fig. 1) during the high water stage period. In addition, two wastewater samples were collected at Yibin (UWW1) and Wuhan (UWW2) in the upper and Middle Reaches, respectively (Fig. 1). Between 10 and 20 l of water were collected in acid-washed containers and were filtered a few hours after their collection on pre-washed 0.2 μm Sartorius® cellulose acetate filters. The first liter was discarded and the following ones were stored in acid-washed polyethylene bottles for analysis after acidification to pH = 2 with bi-distilled HCl. The suspended particulate matter (SPM) collected on the filters were removed in the clean laboratory using

Millipore® Milli-Q water and the solution containing the SPM were gently evaporated at 55 °C. After drying, SPM samples were crushed in an agate mortar.

3.2. Boron concentration and isotopic composition analysis

3.2.1. Dissolved load

B concentrations were measured by isotopic dilution (ID) using the ^{10}B enriched standard solution NIST SRM 952 with a precision better than 1%. The B isotopic determination in water samples is adapted from the method published by Lemarchand et al. (2002a,b). Boron is extracted from water samples by ion exchange using the boron specific resin Amberlite IRA 743. Samples are successively processed through 3 ion chromatography steps using columns containing 50, 10 and 3 µl of resin, respectively. Before loading the sample onto the resin bed, its pH is adjusted to 7–9 and the resin is conditioned by addition of ultra-pure H_2O (Millipore Milli-Q purification system). The resin is then rinsed using sequentially H_2O, NaCl 0.6 M and H_2O. Boron is eluted by loading HCl 0.1 M. The ion chromatography steps allow us to reduce the volume containing B down to 40 µl.

This extraction and purification step is then followed by the "microsublimation technique" (Gaillardet et al. (2001)) in order to separate boron from organic compounds, originating from samples and from the breakdown of the resin. A final organic-free volume of 40 µl is then evaporated. The blank for the total purification procedure is 3.5 ± 1.5 ng B and represents less than 2% of boron sample. Boron isotopic compositions are determined by Positive Thermal Ionisation Mass Spectrometry (PTIMS) on a GV spectrometer using the cesium metaborate method modified from Lemarchand et al. (2002a,b) and Xiao et al. (2007). Measured isotopic compositions are corrected from ^{17}O contribution isotopes as following: $(^{11}B/^{10}B_{corrected}) = (^{11}B/^{10}B_{measured}) - 0.00079$. Results are reported as deviation from the standard NIST SRM 951 boric acid processed through the purification procedure and expressed in δ unit as following:

$$\delta^{11}B = (R_{sample}/R_{std} - 1) \times 1000 \quad (1)$$

where R_{sample} is the $^{11}B/^{10}B$ ratio measured in sample and R_{std} is the $^{11}B/^{10}B$ ratio of the standard processed through the purification procedure The mean value calculated for standard solutions processed through the purification procedure is 4.05042 ± 0.00138 (2σ).

3.2.2. Solid suspended load

B was extracted from the silicate matrix by alkali fusion (Musashi et al., 1990; Tonarini et al., 1997). About 50 mg of fine powdered sample is mixed in a Pt crucible with K_2CO_3 as fluxing agent in the proportion of 1:7. The mixture is brought to a temperature of 950 °C in a muffle furnace for 15 min. After cooling, the fusion glass is dissolved with 30–40 ml of hot water. At this step, dissolution is not total and carbonates precipitate (Tonarini et al., 1997). The water insoluble phase is dissolved in HCl 2N and the pH of the final solution is adjusted to 1. During the neutralization and pH adjustment of the solution, no flocculation of silica gel is observed and dissolution is total. An aliquot of solution, typically 5 ml for the analysis of SPM, is passed through a first column filled with 1 ml of cation exchange resin AG50W-X8. Then, the eluted volume is treated as described for the water samples. The total blank including the fusion step and the chemical purification averages 35 ± 5 ng. The origin of the B contamination is probably related to the crucible itself as highlighted by the correlation between the blank level and the mass of Pt lost during the fusion step (Appendix A). Nevertheless, the blank is negligible compared to the amount of boron extracted from the SPM samples ([B] ≈ 50 ppm) and accounts for less than 3% of the total B extracted for the sample showing the lowest concentration (25 ppm). External reproducibility was evaluated by analyzing the JB2 rock standard and the mean isotopic composition measured during this study is $7.95 \pm 0.48‰$ (2σ, $n = 5$). B concentrations were measured by ID with a precision better than 2% and by colorimetry (Xiao et al., 2007) with a precision of 8% estimated on the replicated analysis of the LKSD2 standard (64 ± 5 ppm, provisional value 65 ppm).

Major elements concentration (Al, Ca, Na, Mg and K) were measured by ICP-OES after digestion in HF-HNO_3-$HClO_4$ acids mixture. Accuracy and reproducibility were determined by analysing ($n = 8$) a national standard (GSD4). Accuracy evaluated as (Xmeas-Xstd)/Xstd with Xmeas the measured concentration and Xstd the recommended value, is better than 5% for all elements excepted for K (12%). Reproducibility is generally better than 10% excepted for Na (11%).

4. RESULTS

4.1. Dissolved load

4.1.1. Boron concentrations

For the Changjiang main channel, B concentrations range from 1.55 µmol/L (M12) to 8.23 µmol/L (M1) (Table 1) and on the whole decrease from upstream to downstream following the same pattern as Na and Cl (Chetelat et al., 2008). Lemarchand et al. (2000) and Lemarchand et al. (2002a,b) report boron concentrations ranging from 1.02 to 1.27 µmol/L for the Changjiang main channel at Nanjing (Fig. 1) lower than the value of 1.76 µmol/L measured at Datong (M16) during this study. Samples collected in the different tributaries present B concentrations ranging from 0.52 µmol/L for the Poyang Lake (T10) to 2.26 µmol/L for the Minjiang (T2) (Table 1). The lowest concentrations are measured for the rivers of the Poyang Lake area draining mainly silicate rocks (0.52–0.75 µmol/L) and rivers of Dongting Lake area draining mainly carbonate rocks (0.59–1.01 µmol/L) as well as for the Jialingjiang (0.63 µmol/L). With the exception of the Changjiang Upper Reach which is clearly impacted by evaporite dissolution (Chen et al., 2002; Chetelat et al., 2008) and shows the highest B concentration, lithological variations (carbonate vs silicate) do not seem to exert a strong control on the dissolved boron content. Boron concentrations are well correlated with Na ($R^2 = 0.87$) and Cl ($R^2 = 0.75$) concentrations whereas they present no relationship with other major elements.

Table 1
Boron concentrations and isotopic compositions of the dissolved and solid loads from the Changjiang basin rivers.

	River	Sample[a]	Location	Latitude	Longitude	Basin area	Water discharge	SPM	Dissolved load			Suspended particulate mater						
									TDSsil[b]	B	δ^{11}Bdis	Al	Ca	K	Mg	Na	B	δ^{11}B
						10^4 km^2	m^3/s	mg/l	mg/l	μmo/l	‰	%	%	%	%	%	ppm	‰
Main channel																		
Upper Reach	Changjiang	M1 (CJ1)	Panzhihua	26°34.503′	101°37.551′			197	10	8.13	2.0	8.05	6.91	2.69	1.76	0.78	82	−11.4
	Changjiang	M2 (CJ3)	Panzhihua	26°34.549′	101°51.109′			103	10	3.30	2.1	8.20	4.91	2.73	2.56	0.71	na	na
	Changjiang	M3 (CJ4)	Yibin	28°42.164′	104°33.385′			748	9	nd	1.7	8.23	4.31	2.57	2.59	0.53	84*	−7.8
	Changjiang	M4 (CJ6)	Yibin	28°46.074′	104°40.316′			376	12	3.56	1.5	8.43	5.06	2.70	2.73	0.71	na	na
	Changjiang	M5 (CJ7)	Luzhou	28°52.180′	105°25.921′			330	12	3.70	3.0	7.28	6.06	2.59	2.53	0.71	na	−8
	Changjiang	M6 (CJ8)	Luzhou	28°54.801′	105°27.897′			241		3.78	1.4	6.95	5.60	2.24	2.40	0.73	na	na
	Changjiang	M9 (CJ12)	Fuling	29°46.270′	107°25.265′			279		2.89	1.7	7.94	4.63	2.20	2.81	0.55	62*	−10.5
	Changjiang	M8 (CJ14)	Chongqing			86.7	8602		5	3.51	5.3	8.50	3.97	2.75	2.21	0.68	71*	−10.5
	Changjiang	M7 (CJ17)	Chongqing	29°32.979′	106°34.173′					3.32	1.6	8.31	4.61	2.60	2.32	0.65	na	na
	Changjiang	M10 (SX3)	TGD reservoir							3.58	2.9	9.49	2.97	3.44	1.91	0.67	na	na
	Changjiang	M11 (SX5)	TGD reservoir					15	8	3.47	1.1	9.20	3.74	3.09	2.12	0.54	na	na
	Changjiang	M12 (SX4)	Yichang			100	8895	4	8	1.56	3.5	10.04	2.77	3.21	2.10	0.59	na	na
Middle/Lower Reaches	Changjiang	M13 (CJ60)	Yueyang	29°38.079′	113°18.739′	125	16,719	40	4	1.83	2.1	na	na	na	na	na	71*	−10.2
	Changjiang	M14 (CJ48)	Wuhan	30°27.397′	114°11.814′			48		2.31	1.4	8.10	2.06	2.35	1.40	0.55	na	na
	Changjiang	M15 (CJ52)	Wuhan	30°40.747′	114°29.876′	149	19,761	48	8	2.27	1.7	8.36	2.32	2.51	1.47	0.62	62*	−7.7
	Changjiang	M16 (CJ36)	Datong			170	27,429	47	5	1.76	3.5	9.81	1.38	2.65	1.48	0.57	76	−10.5
Tributaries																		
Upper Reach	Yalongjiang	T1 (CJ2)	Panzhihua	26°40.127′	101°49.200′	12.8		23	7	1.66	−2.3	16.19	5.76	3.89	3.44	2.97	25	−6
	Minjiang	T2 (CJ5)	Yibin	28°48.779′	104°33.721′	13.6	2596	354	12	2.26	4.5	8.40	4.02	2.94	2.28	0.88	87*	−10.2
	Jialingjiang	T3 (CJ9)	Chongqing	29°33.902′	106°28.632′	15.8	818	6	7	0.63	6.5	3.07	1.32	1.03	0.63	0.22	na	na
	Wujiang	T4 (CJ11)	Fuling	29°41.868′	107°24.486′	8.72	534	10	4	1.27	0.7	na	na	na	na	na	na	na
Middle/Lower Reaches	Yuanjiang	T5 (CJ31)	Taoyuan	28°54.333′	111°29.146′	8.92	870			0.59	14.6	na	na	na	na	na	na	na
	Xiangjiang	T6 (CJ33)	Changsha	28°07.364′	112°56.795′	9.47	2591	21	2	0.84	8.9	10.84	0.67	2.49	0.93	0.25	77*	−9
	Donting Hu	T7 (CJ59)		29°22.625′	113°04.721′	25.94	7026	43		1.01	4.0	9.76	0.71	2.62	1.09	0.31	75*	−9.6
	Ganjiang	T9 (CJ34)	Nanchang	28°40.206′	115°52.053′	8.09	2236	10	4	0.75	5.9	10.31	0.25	2.74	0.80	0.26	50*	−9
	Poyang Hu	T10 (CJ43)		29°38.658′	116°12.224′	16.22	6137	111		0.52		11.67	0.38	2.76	0.89	0.24	na	na
	Hanshui	T8 (CJ47)	Wuhan	30°35.802′	114°04.845′	15.9	1306	59	10	1.80	2.8	7.58	1.63	2.15	1.34	1.05	67	−10
Waste water		UWW1 (YBWS)	Yibin							3.70	8.7							
		UWW2 (CJ58)	Wuhan							4.44	1.7							

[a] In brackets, samples labeling as reported in Chetelat et al. (2008).
[b] Cationic TDS (Total Dissolved Solids) derived from silicate weathering. Data are from Chetelat et al. (2008).
* Measured by colorimetry, other concentrations were measured by isotopic dilution.

4.1.2. Boron isotopic compositions

Rivers of the Changjiang basin present a large range of B isotopic composition, from −2‰ for the Yalongjiang (T1) to +14.6‰ for the Yuanjiang (T5) whereas the Changjiang main channel displays a narrower range from +1.1‰ (M11) to +5.3‰ (M8) (Table 1), similar to that reported by Lemarchand (2001), from +1.7‰ to +4.2‰. With the exception of the Yalongjiang characterized by the lowest isotopic composition associated to a relatively high B concentration (1.66 μmol/L), the $\delta^{11}B$ values tend to increase with the decrease of B concentrations (Fig. 3). The highest $\delta^{11}B$ values are observed for the rivers of the Dongting Lake and Poyang Lake areas with values ranging from +4‰ to +14.6‰. Rivers draining mainly carbonate rocks, namely the Wujiang (T4), Hanshui (T8) and rivers from the Donting Lake area (Figs. 1 and 2) display a large range of boron isotopic composition from +0.7‰ to +14.6‰ which almost covers the range of variation observed for the whole basin whereas the Ganjiang which drains mainly silicate (Figs. 1 and 2) is characterized by a relatively high $\delta^{11}B$ value of +5.9‰. Thus, with these only data, it is not possible to conclude on a lithological control of the boron isotopic composition of river water.

4.2. Solid load

Boron concentrations in the suspended particulate matter (SPM) range from 25 ppm (Yalongjiang, T1) to 87 ppm (Minjiang, T2) with an average value of 68 ppm (Table 1). SPM samples display $\delta^{11}B$ values from −11.4‰ (Changjiang, M1) to −6‰ (Yalongjiang, T1) and are close to the composition reported for sediments of the Mississippi river (Spivack et al., 1987) and for silicate rocks (Palmer and Swihart, 1996 and references therein). The average isotopic composition, −9‰, is close to the value of −7‰ reported by Chaussidon and Albarède (1992) for the continental crust.

5. SOURCES OF DISSOLVED BORON

5.1. Atmospheric inputs

Although continental rainwater displays low boron concentrations (Demuth and Heumann, 1999; Rose et al., 2000; Rose-Koga et al., 2006; Chetelat et al., 2009), 0.09–0.18 μM on average, contribution of atmospheric inputs can be significant for diluted rivers (Rose et al., 2000; Chetelat and Gaillardet, 2005; Lemarchand and Gaillardet, 2006), no data are available for the Changjiang basin. Rose et al. (2000) report an average B concentration of rainwater samples collected in Central Nepal of 0.13 μM. Assuming that they are also representative of the Qinghai–Tibetan Plateau, the part of B derived from atmospheric inputs in the Upper Reach of the Changjiang should be negligible. For other samples, we will assume a mean B concentration in rainwater around 0.18 μM (2 ppb), close to the B concentration observed in other continental locations that we will normalize to the Na concentrations measured in Chinese rainwater and reported in Larssen et al (1999). The deduced average Na/B molar ratio is around 140. In the following discussion, we will use this value to correct B concentrations from atmospheric inputs. The B isotopic composition of rainwater is highly variable ranging from −13‰ to +48‰ and as B concentrations usually decrease with distance from the coast (Rose-Koga et al., 2006). Because rivers from the Donting and Poyang Lakes area display the lowest boron concentrations (Fig. 1, Table 1), they are probably the most influenced by the atmospheric inputs. As the boron isotopic compositions of these river waters are generally higher than that of other samples, this observation is in favor of a relatively high B isotopic composition for the rainwater end-member. Such hypothesis is also supported by the distribution of the data in a $\delta^{11}B$ vs Na/B diagram (Fig. 4) where the highest isotopic composition of 14.6‰ is linked to a Na/B molar ratio of 140, close to the value estimated for rainwater.

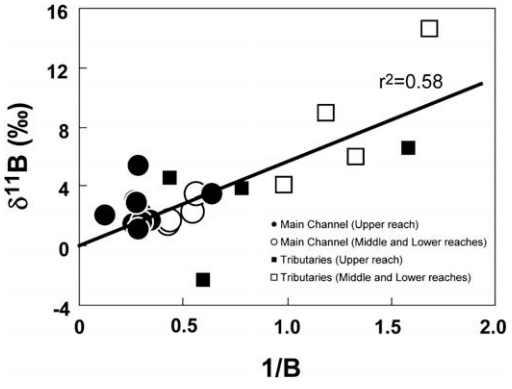

Fig. 3. Relationship between the boron isotopic composition of the dissolved load and the inverse of the boron concentration expressed in μmol/L.

5.2. Contribution of carbonate

Carbonate dissolution is generally the main source of solutes for the rivers of the Changjiang basin (Chen et al., 2002) and contributes from 40% to 80% to the cationic TDS (Chetelat et al., 2008). Compared to marine carbonate, continental carbonate rocks display relatively low boron contents, generally from 1 to 5 ppm (Spivack and You, 1997; Chetelat and Gaillardet, 2005). Assuming that all the calcium present in rivers is derived from carbonate weathering and assuming a B concentration of 5 ppm for carbonates rocks, contribution of carbonate weathering to the dissolved boron budget is generally lower than 3% with the exception of the Jialingjiang (T3) for which the contribution reaches 8%. These estimates are the upper limits for the carbonate contribution, thus we will assume that it is negligible. Similar findings are reported in the case of Himalayan rivers (Rose et al., 2000) and for the Mackenzie basin also dominated by carbonate weathering (Lemarchand and Gaillardet, 2006).

5.3. Evaporite dissolution

The impact of evaporite dissolution to the dissolved load of the Changjiang basin's rivers is highly variable. For the Changjiang main channel, evaporite (essentially halite) weathering accounts for around 45% of the cationic TDS

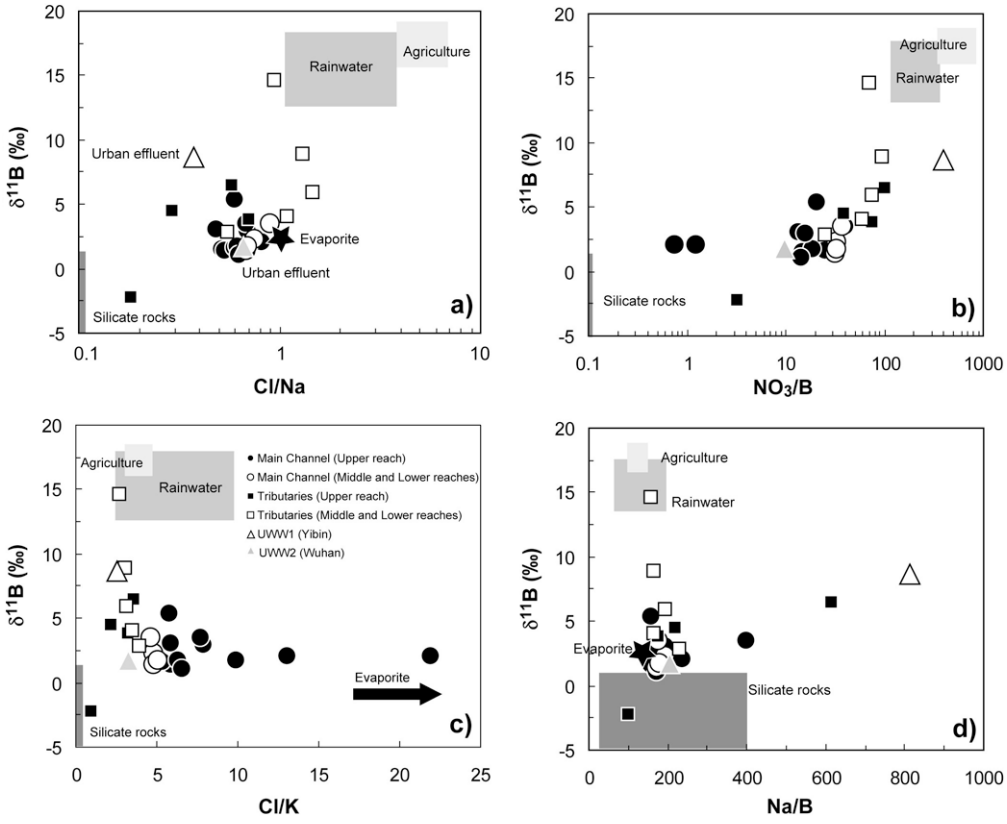

Fig. 4. Relationships between the isotopic compositions of dissolved boron measured in the rivers of the Changjiang basin with some elemental ratios. The range of Na/B molar ratios for the silicate end-member is deduced from the concentrations measured in shale and loess samples reported in Hu and Gao (2008). For the other end-members, see text.

in the Upper Reach (M1) and their contribution falls to less than 10% for the Lower Reach (M16) (Chetelat et al., 2008). Because evaporite display high boron concentrations, their impact on the dissolved B budget may be important as observed for the sample M1 and as highlighted by the correlations between B and Na or Cl concentrations. Sample M1 is characterized by a Cl/B molar ratio of 140 and a relatively low B isotopic composition of +2‰. This last value is in the range of the B isotopic compositions measured by Wang et al. (2001) for the borates of the Qinghai–Tibetan Plateau. These authors report B isotopic compositions ranging from −29.5‰ to +3‰ (median −4‰) and conclude on the non-marine origin of the evaporite.

Rivers of the Changjiang basin are also characterized by high dissolved sulfate concentrations (Chetelat et al., 2008) derived from gypsum dissolution but also from the oxidation of sulfide and atmospheric depositions (Chen et al., 2002; Han and Liu, 2004; Chetelat et al., 2008). Assuming that all SO_4 concentrations result from gypsum weathering and taking the same SO_4/B ratio of 8000 used by Lemarchand and Gaillardet (2006), the maximum contributions of gypsum to the dissolved load never exceed 10%. The higher values are estimated for the Wujiang (6%) and the Jialingjiang (9%), for other samples the contributions range from 0.5% to 4% and thus, the contribution of gypsum dissolution to the dissolved B budget can be neglected.

5.4. Anthropogenic inputs

B can be very sensitive to human activities and numerous studies used boron as a tracer of anthropogenic inputs to groundwater and surface water. Moreover, B isotopic compositions are a powerful tool to decipher the sources of contamination and discriminate between B derived from domestic/industrial effluents and from agricultural practices (Chetelat and Gaillardet, 2005).

The Changjiang basin is faced with a growing anthropogenic pressure (Fu et al., 2007) that affects water quality among other things. On a long term scale, the Changjiang has experienced an increase of the contribution from human activities to the chemical composition of the rivers dissolved load (Chetelat et al., 2008). In the course of this study we have analysed the composition of two urban waste water samples collected in the upper (UWW1) and middle (UWW2) reaches of the Changjiang (Fig. 1). Whereas these two samples present similar chemical compositions regarding major elements, the Na/B ratios and $\delta^{11}B$ are quite different (Table 1). The UWW2 sample is characterized by a Na/B ratio around 800 and a $\delta^{11}B$ of +8.7‰ while UWW2 displays a Na/B ratio of 200 and a B isotopic composition of +1.7‰. In the following discussion, we will assume that the B signatures of either UWW1 or UWW2 are representative of domestic/industrial effluents for the whole basin and test the influence of the choice of the domestic/

industrial end-member on the proportions of dissolved boron derived from the different sources.

Farming is well developed in the Changjiang watershed and paddy fields are abundant in the Sichuan basin as well as in the middle and Lower Reaches. The raise of nitrate concentrations along the Changjiang main channel (Chetelat et al., 2008) from upstream to downstream suggests the importance of agricultural practices on water quality. Water affected by farming shows habitually high Cl/Na ratio and NO_3/Na ratios (Roy et al., 1999). This is obviously the case for rivers of the Dongting and Poyang Lakes catchments for which the Cl/Na ratio may be greater than that of sea-salts (Fig. 4). Because boron can be present in fertilizers as major or trace component, impacts of farming on the dissolved boron budget need to be evaluated for rivers draining agricultural regions. Chetelat and Gaillardet (2005) report B isotopic compositions of +16‰ and +17‰ measured in K and N-fertilizers and a Na/B ratio for water impacted by agricultural practices of 130 ± 20.

5.5. Silicate weathering

In the case of the Changjiang and its tributaries, estimation of the fraction of dissolved boron derived from silicate weathering is not precise because of the potential contribution of the numerous sources of boron mentioned above. Furthermore, the composition of the silicate end-member is probably not unique in term of Na/B (close to 250 for the upper continental crust, based on the B concentration estimated by Hu and Gao (2008) and Na concentration reported by Wedepohl (1995)) or B isotope ratios as shown in the case of Himalayan rivers (Rose et al., 2000) and rivers of the Mackenzie basin (Lemarchand and Gaillardet, 2006). These two studies report a huge range of isotopic compositions for the estimated fraction of boron derived from silicate weathering, between −7‰ and +37‰ in the case of Himalaya and from −2‰ to +30‰ for the rivers of the Mackenzie basin that the authors explain by isotopic fractionations occurring in soils (Rose et al., 2000) or during water/rock interactions in groundwater (Lemarchand and Gaillardet, 2006). We attempted to estimate the proportion of dissolved boron coming from silicate weathering, noted B_{sil}, as well as its isotopic composition, noted $\delta^{11}B_{sil}$ by subtracting the contribution of other sources. In this aim, we used the approach expounded in Chetelat et al. (2008) based on mass balance equation solved by an inversion method (Negrel et al., 1993; Roy et al., 1999; Millot et al., 2003; Chetelat and Gaillardet, 2005). To the initial set of mass balance equations normalized to Na relying on major elements and Sr isotopic data, we added two mixing equations for boron and its isotopes:

$$\left(\frac{B}{Na}\right)_{river} = \sum_i \left(\frac{B}{Na}\right)_i \times \alpha_i(Na) \quad (2)$$

$$(\delta^{11}B)_{river} \times \left(\frac{B}{Na}\right)_{river} = \sum_i (\delta^{11}B)_i \times \left(\frac{B}{Na}\right)_i \times \alpha_i(Na) \quad (3)$$

Where α_i(Na) represents the mixing proportion of Na from the different sources (i = atmosphere, agriculture, domestic/industrial effluents, silicate and evaporite). In this approach, all the parameters are considered as unknown and are affected by error bars which reflect the knowledge of each parameter. The least known are the proportions of Na coming from the different sources. Then, the algorithm adjusts the different parameters from a set of *a priori* values by successive iterations that best fit the whole set of equations. As the B/Na molar ratio and B isotopic compositions of the different sources other than the silicate end-member are assumed to be well known, the addition of these two mass balance equation is not expected to give more constraints on the α_i(Na) calculated in Chetelat et al. (2008) by only using major elements and Sr isotopic ratios.

With the exception of the domestic/industrial end-member (see the discussion above), we supposed that the composition of sources other than silicate was fairly constant in the whole basin. Because of the variability of the B isotopic composition measured in evaporite (Wang et al., 2001) and the lack of constrain on their Na/B ratio, we assumed that the boron present in the sample the most impacted by evaporite contribution (M1) was entirely derived from evaporite dissolution. Thus, we assigned to the evaporite end-member composition a Na/B molar ratio of 140 ± 10 equal to the Cl/B molar ratio measured in sample M1 and a $\delta^{11}B$ of $+2 \pm 0.4$‰ (Table 2). Hence, we did not attempt to estimate B_{sil} and $\delta^{11}B_{sil}$ for samples M1 and M2 characterized by the highest contribution of evaporite (Chetelat et al., 2008). For the atmospheric and agricultural inputs, we assumed Na/B molar ratios of 140 ± 70 and 140 ± 20 and B isotopic compositions of $+15 \pm 3$‰ and $+17 \pm 2$‰, respectively (Table 2). We supposed that these end-members were well constrained compared to the silicate source for which the Na/B ratio and isotopic composition are free to vary around 250 and 0‰, respectively.

During this study, we have neglected the impact of vegetation and biological uptake on the boron biogeochemical cycle. Because boron is an important nutrient, impact of vegetation on its cycle may be important as it was highlighted for some forested catchments (Hogan and Blum, 1998; Bouchez et al., 2006). In the case of Si, biological uptake was evocated by Ding et al. (2004) to explain the evolution of the Si isotopic composition along the Changjiang main channel. However, no decisive argument was given by the authors.

Table 2
Boron signatures of the different end-members used in the calculation of the fraction of dissolved boron derived from silicate weathering.

	Atmosphere	Agriculture	Domestic/industrial effluents		Evaporate
			UWW1	UWW2	
Na/B (molar ratio)	140 ± 70	140 ± 20	833 ± 50	204 ± 12	140 ± 10
$\delta^{11}B$ (‰)	$+15 \pm 3$	$+17 \pm 2$	$+8.3 \pm 0.4$	$+1.7 \pm 0.4$	$+2 \pm 0.4$

This issue would need to be investigated in details but in the present study it is difficult to evaluate the role of biological processes on the boron budget of the Changjiang basin rivers.

In addition, these mass balance equations implicitly assume that B is conservative in rivers and that B partition between solid and dissolved loads is not further controlled by adsorption onto solid surface (Rose et al., 2000; Chetelat and Gaillardet, 2005; Lemarchand and Gaillardet, 2006). By taking the same value (≈20) reported by Lemarchand and Gaillardet (2006) for the partition coefficient (Kd) between adsorbed and dissolved boron, the proportion of soluble boron adsorbed onto solid surface calculated for a range of SPM concentrations between 100 and 400 mg/l is less than 1% and thus is negligible.

5.6. Sensitivity of B_{sil} and $\delta^{11}B_{sil}$ to the choice of the urban/industrial end-members

We now test the influence of the choice of the domestic/industrial end-member on the calculated fraction of dissolved boron derived from silicate weathering and its isotopic composition by assuming that either UWW1 or UWW2 is representative of the urban/industrial inputs for the whole basin. Composition of other end-members is identical to that reported Table 2. For two samples located in the Upper Reach, M12 and T3, the fraction of B derived from silicate weathering is either negative when calculated using UWW2 as end-member or displays a too large uncertainty to be considered when calculated using UWW1. For other samples, the relative difference between the two estimations is in average around 45% with the exception of M13 for which the relative difference reaches 80% (Appendix B). Note that given the uncertainties, the proportions of boron derived from atmospheric inputs, agricultural inputs and evaporite weathering are not influenced by the choice of the domestic/industrial end-member. In the estimation of the proportion of dissolved boron derived from the different sources, we will consider the average of the two estimations.

Considering the propagated uncertainties on other end-members, the two calculations give similar results for the isotopic composition of dissolved boron derived from silicate weathering (Appendix B).

5.7. Sensitivity of B_{sil} and $\delta^{11}B_{sil}$ to the choice of the atmospheric and evaporite end-members

We also performed a series of sensitivity tests to assess the dependence of the results on the choice of the atmospheric end-member. In a first series, we fixed the B/Na ratio and the B isotopic composition around the values reported by Rose et al. (2000), 0.006 and +5.5‰, respectively. Whereas the fraction of B derived from silicate weathering is similar between the two calculations, the B isotopic compositions are shifted toward higher values by 0.5–3‰ for the most sensitive samples and on average by 1.5‰. This last value is typically the uncertainty we get on the isotopic composition of B_{sil} by running the inversion model. In the second series, we fixed the isotopic composition of the atmospheric end-member at 25‰ and keep unchanged the B/Na ratio (0.007). The B isotopic composition of the fraction of boron derived from silicate weathering is shifted toward lower values by again 0.5–3‰. Conversely, if we fix the B isotopic composition at 15% and vary the B/Na ratio, for example a B/Na ratio twice as that we used, the relative difference between the amount of B derived from silicate weathering vary from less than 5–27%, and is on average around 12%. Regarding the isotopic compositions, $\delta^{11}B_{sil}$ are shifted toward lower values by 0.1–4‰ for the most sensitive sample and on average by 1.8‰.

Hence, a couple of samples are relatively sensitive to the choice of the atmospheric end-member but generally the influence of the choice of atmospheric end-member is limited. Furthermore, variations of the composition of the atmospheric inputs are mostly taken into account into the uncertainties affected to the B/Na ratio and $\delta^{11}B$ value (Table 2).

To test the influence of the composition of the evaporite end-member, we performed some sensitivity tests by varying the Na/B ratio and $\delta^{11}B$ value of the evaporite end-member. We fixed other parameters to the values shown in Table 2 (here UWW1 is assumed to be representative of the urban/industrial inputs for the whole basin) and we chose a Na/B ratio of 0.0035 (half of the initial value) and an isotopic composition of −4‰ (median of the values reported for the borate minerals) for the evaporite end-member. With the exception of T3 and M12 for which the relative difference between the amount of B derived from silicate weathering is 62% and 133%, respectively, for other samples the relative difference is on average around 15%. The isotopic compositions of the fraction of B derived from silicate weathering are shifted toward higher values by 0.2–1.6‰.

Hence, with the exception of T3 and M12 which are strongly dependent on the choice of the evaporite end-member, for other samples, given the uncertainties, the results between the two calculations are similar

6. CONTRIBUTION OF SILICATE WEATHERING TO THE BORON RIVERINE BUDGET

As expected, contribution of atmospheric depositions is relatively low, accounting for less than 10% of the total dissolved B with the exception of the Wujiang (T4) and Ganjiang (T9) for which the contribution reaches $14 \pm 6\%$ and $16 \pm 9\%$, respectively (Fig. 5a and b). Contribution of evaporite to the dissolved boron budget is relatively important for the Changjiang main channel and range from $24 \pm 10\%$ to $31 \pm 7\%$ (Fig. 5a). For the main tributaries, the contribution of evaporite range from $8 \pm 1\%$ to $25 \pm 11\%$ (Fig. 5b). Anthropogenic (including domestic/industrial and agricultural inputs) inputs account between $17 \pm 10\%$ and $28 \pm 16\%$ of the total dissolved boron for the main channel (Fig. 5a) and from 0% to $36 \pm 16\%$ for the main tributaries (Fig. 5b). In the case of the Changjiang main channel the proportion of dissolved boron derived from silicate weathering varies from $40 \pm 17\%$ to $50 \pm 10\%$ (Fig. 5a) whereas for the main tributaries

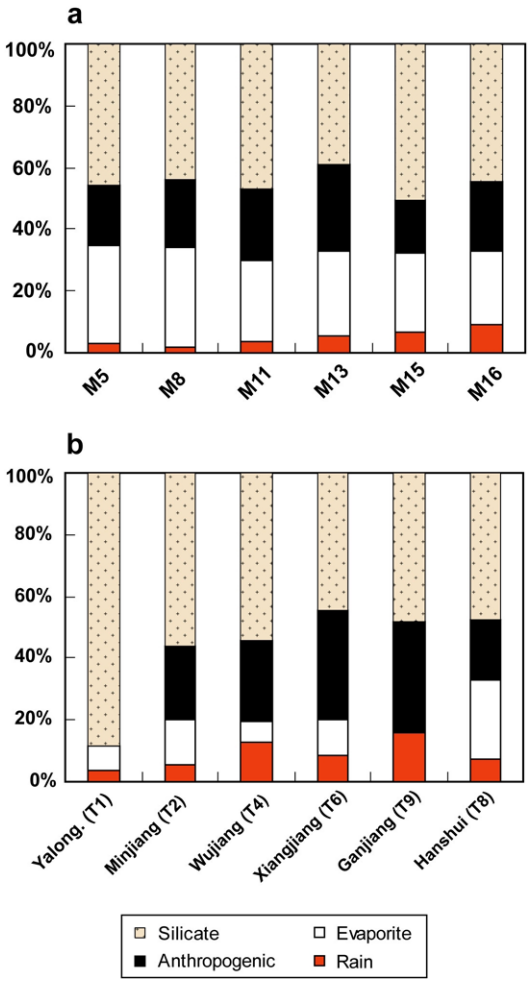

Fig. 5. Calculated contributions of the different sources to the dissolved boron budget with the inversion method for the Changjiang main stream at different locations (a) and the major tributaries (b). The proportions of dissolved boron derived from the different sources are calculated from the average of the two estimates for the fraction of B derived from silicate weathering and domestic/industrial inputs (Appendix B). The anthropogenic contribution includes the agricultural and the domestic/industrial inputs.

(Fig. 5b) the silicate weathering accounts between $45 \pm 8\%$ and 88% of the dissolved boron load.

Hence, with the exception of few singular samples, B dissolved budget for the Changjiang basin rivers is dominated by silicate weathering which accounts on average for 45–50% of the total dissolved boron.

Regarding the B isotopic compositions, the $\delta^{11}B$ of the dissolved load range from $-3‰$ to $+9‰$ (Appendix B) on the whole basin and are higher than that the isotopic composition of the continental crust (Chaussidon and Albarède, 1992). At Datong, the most downstream hydrological station not influenced by tidal phenomenon, the B isotopic composition of the silicate fraction reaches $+0‰$. Based on the monthly water discharge for August 2006 and the calculated concentration of dissolved B derived from silicate weathering ($B_{sil.}$), we estimate a flux of 7500 ± 1300 tB/yr accounting for $44 \pm 9\%$ of the total dissolved boron flux.

7. BORON ISOTOPE BEHAVIOUR DURING SILICATE WEATHERING

The fraction of boron derived from silicate weathering is well partitioned between the dissolved and solid load (Fig. 6) with a preference for the dissolved phase. With the exception of the Minjiang (T2) for which the dissolved phase represents only 30%, for other samples the dissolved phase accounts for 70–96% of the total boron derived from silicate weathering. This feature highlights the high solubility of boron during silicate weathering. The dissolved load derived from silicate weathering appears to be systematically enriched in ^{11}B compared with the suspended sediments (Fig. 7). If we note Δ the difference between the isotopic composition of the suspended sediments and the dissolved load (here the average of the two estimates reported in Appendix B) and expressed as,

$$\Delta_{\text{solid-dissolved}} = \delta^{1}1B_{SPM} - \delta^{1}1B_{sil}. \quad (4)$$

Δ values range from $-19‰$ to $-3‰$ and cluster at around $-10‰$. Such enrichment in heavy isotopes of the dissolved load is in agreement with an isotopic fractionation during water/rock interaction which would favor the mobility of the heavy isotope into the fluid and/or the removal of ^{10}B from the solution during secondary processes such as clays formation or preferential adsorption of ^{10}B at solids surface. These values correspond to fractionation factors α between solid and fluid ranging from 0.981 to 0.997 and are higher than those observed during B adsorption onto clay or goethite surfaces, typically from 0.960 to 0.978 (Palmer et al.,1987; Lemarchand et al., 2007). Although the mineralogy of the suspended particulate matter has not been investigated in study, it is likely that suspended sediments contain not only secondary products of weathering such

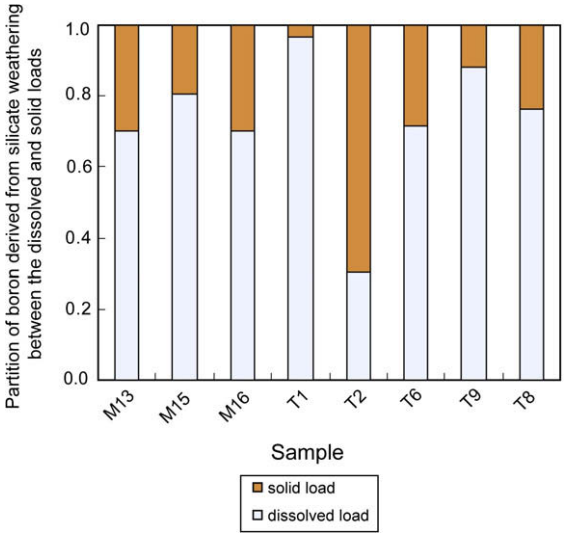

Fig. 6. Partition of boron derived from silicate weathering between dissolved and solid loads.

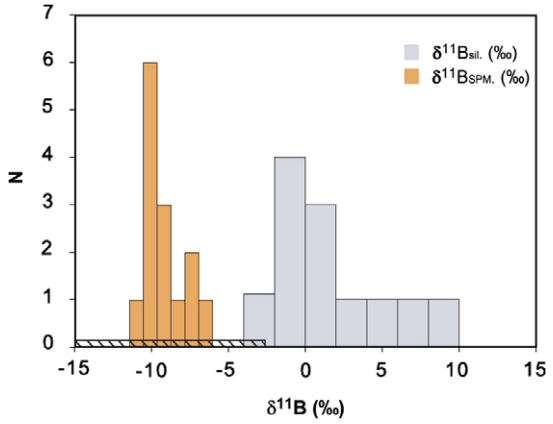

Fig. 7. Histogram of the B isotopic compositions measured in suspended sediments ($\delta^{11}B_{SPM}$) and calculated for dissolved boron derived from silicate weathering ($\delta^{11}B_{sil}$). The range of the isotopic compositions of present Li-rich tourmalines (Chaussidon and Albarède, 1992) is reported for comparison (hatched area). They are assumed to provide an average boron isotopic composition of the continental crust (−7‰).

as clays or oxyhydroxides but also primary minerals. Previous studies (Yang et al., 2002b, 2004) reported the mineralogy of bed sediments and on average quartz, feldspar and mica account for 72% of the total content, clays, mainly illite, account for 19%, heavy minerals for 3% and the last 6% include calcite and dolomite. The occurrence of primary minerals in the suspended load could also explain the observation that the boron isotopic composition of the suspended matter is close to the composition of the continental crust.

Another observation is that when Δ is reported as a function of the Al/B ratio measured in suspended sediments (Fig. 8), samples displaying the lowest Δ values are close or show a slight enrichment of boron relative to the upper continental crust and fall into the range of the Al/B ratios observed in shales (average of the Al/B mass ratio, 0.09×10^4, Hu and Gao, 2008). Conversely, the sample with the highest Δ value is characterized by a loss of boron.

Such an evolution of both Δ values and Al/B ratio may be explained by a difference of the proportions of boron released in solution during silicate weathering. The more boron is mobilized, the more the Al/B ratio of the suspended sediments increases and the isotopic composition of both dissolved and suspended load converge, i.e., Δ tends to 0.

Thus, the relationship between Δ values and the Al/B ratios measured in suspended particulate matter suggests that two competitive processes may control the B isotopic composition of the solid and dissolved loads: (1) Isotopic fractionation which enriches the solution in heavy isotopes by secondary mineral formation and preferential incorporation of ^{10}B in solids (2) dissolution without isotopic fractionation characterized by a loss of boron relative to the bedrock and a similarity between the B isotopic composition of the suspended and dissolved loads.

Such competitive processes between boron leaching and boron incorporation into secondary minerals is supported by the relationship between Δ and the partition coefficient of boron defined as the ratio between the concentration of dissolved boron derived from silicate weathering (B_{sil}) and the boron concentration measured in suspended sediments (B_{SPM}) (Fig. 9). When boron is highly mobilized during silicate weathering i.e., high B_{sil}/B_{SPM} ratio, the isotopic composition of the dissolved load approaches that of the bed rock and Δ tends to 0‰. Whereas, when the proportion of boron released into solution is low, the isotopic composition of the dissolved phase is more fractionated compared to the bedrock and it is enriched in heavy isotope.

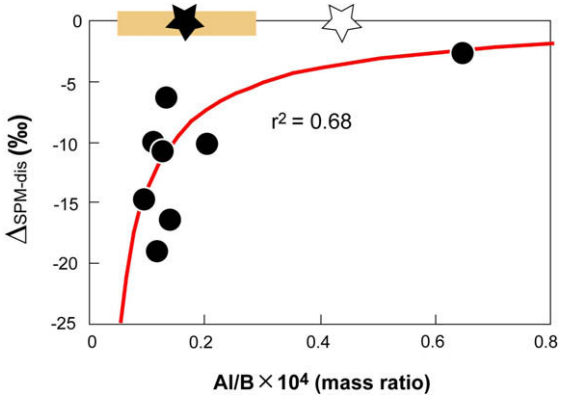

Fig. 8. Evolution of $\Delta_{solid\text{-}dissolved}$ with the Al/B mass ratio measured in suspended sediments. The Al/B ratios of the upper continental crust deduced from Wedepohl (1995) (☆) and Hu and Gao (2008) (★) are reported for comparison. We also report the range of the Al/B mass ratio measured in shales by Hu and Gao (2008) (average value, 0.09×10^4).

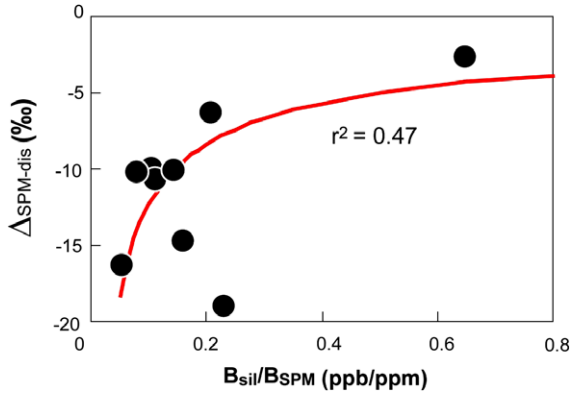

Fig. 9. Evolution of $\Delta_{solid\text{-}dissolved}$ with the partition coefficient of boron during silicate weathering processes. The partition coefficient is defined as the concentration of dissolved boron derived from silicate weathering (B_{sil}) normalized to the boron concentration measured in suspended particulate matter (B_{SPM}). B_{sil} is calculated from the average of the two estimates for the fraction of dissolved boron derived from silicate weathering (Appendix B).

8. CONCLUSIONS

We have measured the B concentrations and B isotopic compositions of both dissolved and solid loads for rivers of the Changjiang basin draining different lithologies under different climates in order to asses the B behaviour during continental erosion. After correction from mainly evaporite and anthropogenic contributions, we showed that silicate weathering contributes between 40% and 88% to the dissolved boron budget and with the exception of a couple of singular rivers is the major source of dissolved boron. Boron is highly mobile during silicate weathering and the dissolved load represents between 30% and 96% of the total flux (including suspended and dissolved loads) of boron derived from silicate weathering. Regarding the isotopic composition, the dissolved load is systematically enriched in heavy isotope compared to the suspended particulate matter with $\Delta_{\text{solid-dissolved}}$ values ranging from $-19‰$ to $-3‰$. The range of $\Delta_{\text{solid-dissolved}}$ values observed for the Changjiang basin rivers can be explained the extent of boron leaching relative to boron uptake into secondary phases. The first process is characterized by a loss of boron relative to the bedrock without apparent isotopic fractionation whereas the last one is associated to a large isotopic fractionation which enriches the dissolved phase in heavy isotope.

ACKNOWLEDGMENTS

The authors thank S.L. Li, J. Li, B.L. Wang, F.S. Wang, X.L. Liu, L.B. Li, H. Ding and J. Guan for their help during the samples collection as well as the staffs of the Datong and Wuhan hydrological stations. Comments and suggestions by J. Schott and two anonymous reviewers greatly improved the quality of the manuscript. This work was supported jointly by the Chinese Academy of Sciences through the International Partnership Project, by the National Natural Science Foundation of China (Grants Nos. 90610037 and 40873012), by the Ministry of Science and Technology of China through the National Basic Research Program of China ("973" Program, Grant No. 2006CB4003200).

APPENDIX A. ORIGIN OF THE BLANK DURING THE B EXTRACTION FROM THE SILICATE MATRIX BY ALKALI FUSION

Blanks were measured for a single series of measurements for different fusion times, 15, 30, 45 and 60 min. The contamination level is correlated with the time of fusion and the amount of Pt lost from the crucible during the fusion step. B is present as trace in the Pt crucible and from the slope of the regression line between the mass of Pt lost during the fusion step and the blank levels, we estimated a B concentration of around 11 ppm for the crucible. The error bars on the blank concentration were estimated based on the replicated analysis of the blank for a fusion time of 15 min (see sampling and analytical section) (Fig. A1).

APPENDIX B. PROPORTION OF DISSOLVED BORON (%) DERIVED FROM THE DIFFERENT SOURCES CALCULATED USING THE END-MEMBER SIGNATURES REPORTED TABLE 2.

	Atmosphere	Agriculture	Evaporite	Domestic/industrial effluents		Silicate		$\delta^{11}B_{sil}$	
				UWW1	UWW2	1[a]	2[b]	1[a]	2[b]
M5	3 ± 1	1 ± 0.5	31 ± 4	7 ± 1	29 ± 3	58 ± 5	36 ± 6	+2.0 ± 0.8	+3.5 ± 1.2
M8	2 ± 1	2 ± 1	31 ± 7	7 ± 2	35 ± 7	55 ± 15	32 ± 12	+6.1 ± 1	+10.9 ± 2
M11	4 ± 2	1 ± 0.5	26 ± 3	9 ± 1	35 ± 3	60 ± 4	34 ± 6	-1.5 ± 1.0	-2.2 ± 1.6
M12	8 ± 5	3 ± 1	61 ± 15	19 ± 7	–	9 ± 27	–	–	–
M13	6 ± 1	1 ± 0.5	26 ± 3	11 ± 1	43 ± 3	56 ± 5	23 ± 7	-0.4 ± 1.3	-0.1 ± 1.9
M15	7 ± 4	3 ± 2	25 ± 3	6 ± 1	23 ± 5	59 ± 12	42 ± 11	-1.3 ± 1.4	-1.5 ± 1.9
M16	10 ± 8	6 ± 3	24 ± 10	6 ± 2	26 ± 8	53 ± 17	35 ± 17	-0.3 ± 2.0	+0.2 ± 2.8
T1	3 ± 2	0	8 ± 1	0	0	88 ± 4	88 ± 4	-3.4 ± 0.7	-3.4 ± 0.7
T2	5 ± 3	2 ± 0.5	15 ± 1	8 ± 1	34 ± 3	69 ± 4	43 ± 6	+3.3 ± 1.0	+5.6 ± 1.3
T3	9 ± 5	14 ± 2	31 ± 5	31 ± 6	–	15 ± 16	–	–	–
T4	14 ± 6	4 ± 2	7 ± 2	10 ± 2	43 ± 3	65 ± 24	33 ± 7	-0.1 ± 1.9	+0.7 ± 3.2
T6	9 ± 6	22 ± 4	11 ± 1	5 ± 2	21 ± 7	53 ± 19	38 ± 11	+6.1 ± 1.8	+8.7 ± 2.5
T8	8 ± 4	4 ± 1	25 ± 11	6 ± 2	26 ± 10	57 ± 15	38 ± 18	+0.0 ± 1.5	+0.3 ± 2.1
T9	16 ± 9	14 ± 3	0	8 ± 2	35 ± 7	61 ± 18	35 ± 15	+0.5 ± 2.5	+1.5 ± 3.7

[a] Calculated using UWW1 as end-member for the domestic/industrial inputs.
[b] Calculated using UWW2 as end-member for the domestic/industrial inputs.

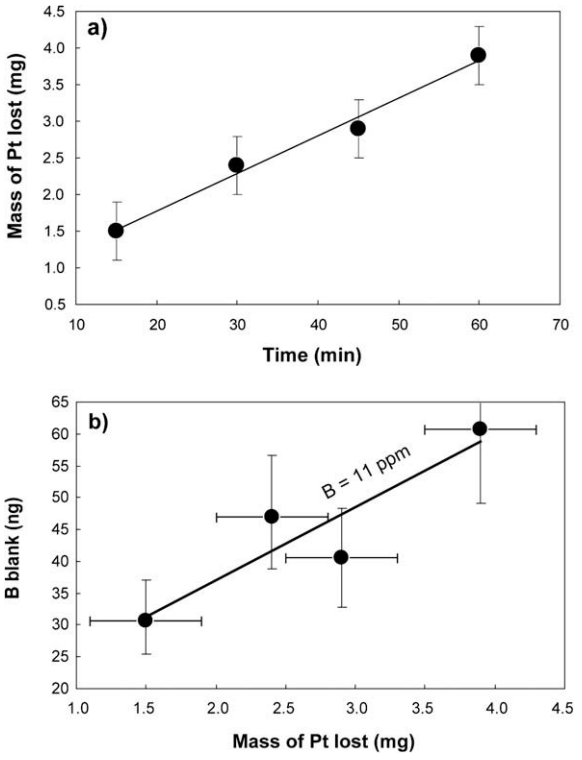

Fig. A1. Evolutions of the loss of Pt from the crucible as a function of the time of fusion (a) and of the B blank level with the mass of Pt lost from the crucible during the fusion (b).

REFERENCES

Baes C. F. and Mesmer R. E. (1976) *The Hydrolysis of Cations*. Wiley.

Berner R. A., Lassaga A. C. and Garrels R. M. (1983) The carbonate-silicate geochemical cycle and its effect on atmospheric carbon-dioxide over the past 100 million years. *Am. J. Sci.* **283**, 641–683.

Bouchez J., Gaillardet J., Chetelat B. and Gerard F. (2006) Boron isotopic fractionation by land plants of a forested ecosystem under temperate climate: consequences for boron global biogeochemical cycle. *GERM workshop*. University of Columbia, New York.

Byrne R. H., Yao W., Klochko K., Tossell J. A. and Kaufman A. J. (2006) Experimental evaluation of the isotopic exchange equilibrium 10B(OH)3+11B(OH)4-=11B(OH)3+10B(OH)4- in aqueous solution. *Deep Sea Res. I Oceanogr. Res. Papers* **53**(4), 684–688.

Chaussidon M. and Albarède F. (1992) Secular boron isotopes variations in the continental crust: an ion microprobe study. *Earth Planet. Sci. Lett.* **108**, 229–241.

Chen Z., Li J., Shen H. and Zhanghua W. (2001) Yangtze River of China: historical analysis of discharge variability and sediment flux. *Geomorphology* **41**(2–3), 77–91.

Chen J., Wang F., Xia X. and Zhang L. (2002) Major element chemistry of the Changjiang (Yangtze River). *Chem. Geol.* **187**(3–4), 231–255.

Chetelat B. and Gaillardet J. (2005) Boron isotopes in the seine river, France. A probe of anthropogenic contamination. *Environ. Sci. Technol.* **39**(8), 2486–2493.

Chetelat B., Liu C. Q., Zhao Z. Q., Wang Q. L., Li S. L., Li J. and Wang B. L. (2008) Geochemistry of the dissolved load of the Changjiang Basin rivers: anthropogenic impacts and chemical weathering. *Geochim. Cosmochim. Acta* **72**(17), 4254–4277.

Chetelat B., Gaillardet J. and Freydier R. (2009) Use of B isotopes as a tracer of anthropogenic emissions in the atmosphere of Paris, France. *Appl. Geochem.* **24**(5), 810–820.

Demuth N. and Heumann K. G. (1999) Determination of trace amounts of boron in rainwater by ICP-IDMS and NTI-IDMS and the dependence on meteorological and anthropogenic influences. *J. Anal. Atomic Spectrom.* **14**(9), 1449–1453.

Ding T., Wan D., Wang C. and Zhang F. (2004) Silicon isotope compositions of dissolved silicon and suspended matter in the Yangtze River, China. *Geochim. Cosmochim. Acta* **68**(2), 205–216.

Fu B. J., Zhuang X. L., Jiang G. B., Shi J. B. and Lu Y. H. (2007) Environmental problems and challenge in China. *Environ. Sci. Technol.* **41**(22), 7597–7602.

Gaillardet J., Lemarchand D., Göpel C. and Manhès G. (2001) Evaporation and sublimation of boric acid: application for boron purification from organic rich solutions. *Geostand. Newsl.* **25**(1).

Georg R. B., Reynolds B. C., Frank M. and Halliday A. N. (2006) Mechanisms controlling the silicon isotopic compositions of river waters. *Earth Planet. Sci. Lett.* **249**(3–4), 290–306.

Godderis Y. and Francois L. M. (1995) The Cenozoic evolution of the strontium and carbon cycles: relative importance of continental erosion and mantle exchanges. *Chem. Geol.* **126**(2), 169–190.

Godderis Y., Donnadieu Y., Nedelec A., Dupre B., Dessert C., Grard A., Ramstein G. and Francois L. M. (2003) The Sturtian 'snowball' glaciation: fire and ice. *Earth Planet. Sci. Lett.* **211**(1–2), 1–12.

Han G. and Liu C.-Q. (2004) Water geochemistry controlled by carbonate dissolution: a study of the river waters draining karst-dominated terrain, Guizhou Province, China. *Chem. Geol.* **204**(1–2), 1–21.

Hogan J. F. and Blum J. D. (1998) Boron isotopic variation in streamwater from a forested catchment. GSA Abstracts with Programs, 277.

Hu Z. and Gao S. (2008) Upper crustal abundances of trace elements: a revision and update. *Chem. Geol.* **253**(3–4), 205–221.

Huh Y., Chan L. H. and Edmond J. M. (2001) Lithium isotopes as a probe of weathering processes: Orinoco River. *Earth Planet. Sci. Lett.* **194**(1–2), 189–199.

Kisakurek B., James R. H. and Harris N. B. W. (2005) Li and delta Li-7 in Himalayan rivers: proxies for silicate weathering? *Earth Planet. Sci. Lett.* **237**(3–4), 387–401.

Larssen T., Seip H. M., Semb A., Mulder J., Muniz I. P., Vogt R. D., Lydersen E., Angell V., Dagang T. and Eilertsen O. (1999) Acid deposition and its effects in China: an overview. *Environ. Sci. Policy* **2**(1), 9–24.

Lemarchand D. (2001) Géochimie isotopique du bore: érosion continentale, bilan océanique et paléo-pH. Ph.D. dissertation, Université Paris 7

Lemarchand D. and Gaillardet J. (2006) Transient features of the erosion of shales in the Mackenzie basin (Canada), evidences from boron isotopes. *Earth Planet. Sci. Lett.* **245**(1–2), 174–189.

Lemarchand D., Gaillardet J. and Lewin É. (2000) The influence of rivers on marine boron isotopes and implications for reconstructing past ocean pH. *Nature* **408**, 951–954.

Lemarchand D., Gaillardet J., Göpel C. and Manhès G. (2002a) An optimized procedure for boron separation and mass spectrometry analysis for river samples. *Chem. Geol.* **182**(2–4), 323–334.

Lemarchand D., Gaillardet J., Lewin E. and Allègre C. J. (2002b) Boron isotope systematics in large rivers: implications for the

marine boron budget and paleo-pH reconstruction over the Cenozoic. *Chem. Geol.* **190**(1–4), 123–140.

Lemarchand E., Schott J. and Gaillardet J. (2005) Boron isotopic fractionation related to boron sorption on humic acid and the structure of surface complexes formed. *Geochim. Cosmochim. Acta* **69**(14), 3519–3533.

Lemarchand E., Schott J. and Gaillardet J. (2007) How surface complexes impact boron isotope fractionation: evidence from Fe and Mn oxides sorption experiments. *Earth Planet. Sci. Lett.* **260**(1–2), 277–296.

Liu S. M., Zhang J., Chen H. T., Wu Y., Xiang H. and Zhang Z. F. (2003) Nutrients in the Changjiang and its tributaries. *Biogeochemistry* **62**, 1–18.

Millot R., Gaillardet J., Dupre B. and Allegre C. J. (2003) Northern latitude chemical weathering rates: clues from the Mackenzie River Basin, Canada. *Geochimica et Cosmochimica Acta* **67**(7), 1305–1329.

Musashi M., Oi T., Ossaka T. and Kakihana H. (1990) Extraction of boron from GSJ rock reference samples and determination of their boron isotopic ratios. *Anal. Chim. Acta* **231**, 147–150.

Negrel P., Allegre C. J., Dupre B. and Lewin E. (1993) Erosion sources determined by inversion of major and trace element ratios and strontium isotopic ratios in river: the Congo Basin case. *Earth Planet. Sci. Lett.* **120**(1–2), 59–76.

Palmer M. R. and Swihart G. H. (1996) Boron isotope geochemistry: an overview. In *Boron: Mineralogy, Petrology and Geochemistry*, vol. 33 (eds. E. S. Grew and L. M. Anovitz). Mineralogical Society of America.

Palmer M. R., Spivack A. and Edmond J. M. (1987) Temperature and pH controls over isotopic fractionation during adsorption of boron on marine clay. *Geochim. Cosmochim. Acta* **51**, 2319–2323.

Raymo M. E., Ruddiman W. F. and Froelich P. N. (1988) Influence of late Cenozoic mountain building on ocean geochemical cycles. *Geology* **16**, 649–653.

Rose E. F., Chausidon M. and France-Lanord C. (2000) Fractionation of boron isotopes during erosion processes: the example of Himalayan rivers. *Geochim. Cosmochim. Acta* **64**(3), 397–408.

Rose-Koga E. F., Sheppard S. M. F., Chaussidon M. and Carignan J. (2006) Boron isotopic composition of atmospheric precipitations and liquid–vapour fractionations. *Geochim. Cosmochim. Acta* **70**(7), 1603–1615.

Roy S., Gaillardet J. and Allegre C. J. (1999) Geochemistry of dissolved and suspended loads of the Seine River, France: anthropogenic impact, carbonate and silicate weathering. *Geochim. Cosmochim. Acta* **63**(9), 1277–1292.

Spivack A. J. and You C.-F. (1997) Boron isotopic geochemistry of carbonates and pore waters, Ocean Drilling Program Site 851. *Earth Planet. Sci. Lett.* **152**(1–4), 113–122.

Spivack A. J., Palmer M. R. and Edmond J. M. (1987) The sedimentary cycle of the boron isotopes. *Geochim. Cosmochim. Acta* **51**, 1939–1949.

Tipper E. T., Galy A. and Bickle M. J. (2006) Riverine evidence for a fractionated reservoir of Ca and Mg on the continents: implications for the oceanic Ca cycle. *Earth Planet. Sci. Lett.* **247**(3–4), 267–279.

Tonarini S., Pennisi M. and Leeman W. P. (1997) Precise boron isotopic analysis of complex silicate (rock) samples using alkali carbonate fusion and ion-exchange separation. *Chem. Geol.* **142**, 129–137.

Tossell J. A. (2006) Boric acid adsorption on humic acids: ab initio calculation of structures, stabilities, 11B NMR and 11B, 10B isotopic fractionations of surface complexes. *Geochim. Cosmochim. Acta* **70**(20), 5089–5103.

Wang Q. Z., Xiao Y. K., Zhang C. G., Wei H. Z. and Zhao Z. Q. (2001) Boron isotopic compositions of some boron minerals in Qinghai and Tibet. *Bull. Mineral. Petrol. Geochem.* **20**(4), 364–366.

Wedepohl K. H. (1995) The composition of the continental crust. *Geochim. Cosmochim. Acta* **59**, 1217–1232.

Xiao Y. K., Li S. Z., Wei H. Z., Sun A. D., Liu W. G., Zhou W. J., Zhao Z. Q., Liu C. Q. and Swihart G. H. (2007) Boron isotopic fractionation during seawater evaporation. *Mar. Chem.* **103**(3–4), 382–392.

Xing G. X. and Zhu Z. L. (2002) Regional nitrogen budgets for China and its major watersheds. *Biogeochemistry* **57**(1), 405–427.

Yang S.-l., Zhao Q.-y. and Belkin I. M. (2002a) Temporal variation in the sediment load of the Yangtze River and the influences of human activities. *J. Hydrol.* **263**(1–4), 56–71.

Yang S. Y., Jung H. S., Choi M. S. and Li C. X. (2002b) The rare earth element compositions of the Changjiang (Yangtze) and Huanghe (Yellow) river sediments. *Earth Planet. Sci. Lett.* **201**(2), 407–419.

Yang S. Y., Jung H. S. and Li C. X. (2004) Two unique weathering regimes in the Changjiang and Huanghe drainage basins: geochemical evidence from river sediments. *Sed. Geol.* **164**(1–2), 19–34.

Associate editor: Jacques Schott